Nuclear Instruments and Methods in Physics Research B 267 (2009) 652–655

Contents lists available at ScienceDirect

Nuclear Instruments and Methods in Physics Research B

journal homepage: www.elsevier.com/locate/nimb

Molecular dynamics simulations to explore the effect of chemical bonding in the keV bombardment of Si with C_{60}, Ne_{60} and $^{12}Ne_{60}$ projectiles

K.D. Krantzman [a,*], B.J. Garrison [b]

[a] Department of Chemistry and Biochemistry, College of Charleston, 66 George Street, Charleston, SC 29424, USA
[b] Department of Chemistry, Penn State University, 104 Chemistry Building, University Park, PA 16802, USA

ARTICLE INFO

Article history:
Received 11 October 2008
Received in revised form 6 November 2008
Available online 24 December 2008

PACS:
68.49.Sf
61.80.Jh
79.20.Ap
79.20.Rf

Keywords:
Molecular dynamics
MEDF
C_{60}
Silicon

ABSTRACT

Depth profiling experiments using secondary ion spectrometry (SIMS) have shown effects that are characteristic to the pairing of the C_{60}^+ projectile with a Si target. Previous molecular dynamics simulations demonstrate that this unusual behavior is due to the fact that strong covalent bonds are formed between the C atoms in the projectile and the Si atoms in the target, which result in the implantation of carbon into the solid. The focus of this paper is to understand how the formation of chemical bonds affects the net sputtered yield. The results of molecular dynamics simulations of the keV bombardment of Si with C_{60}, Ne_{60} and $^{12}Ne_{60}$ at normal incidence are compared over a range of incident kinetic energies from 5 to 20 keV. The net yields with Ne_{60} and $^{12}Ne_{60}$ are significantly greater than with C_{60} at all incident kinetic energies, with $^{12}Ne_{60}$ having the largest values. Application of the mesoscale energy deposition footprint (MEDF) model shows that the initial deposition of energy into the substrate is similar with all three projectiles. Snapshots of the initial pathway of the projectile atoms through the substrate show a similar lateral and vertical distribution that is centered in the region of the energy footprint. Therefore, the reason for the reduced yield with C_{60} is that the C atoms form bonds with the Si atoms, which causes them to remain in the substrate instead of being sputtered.

Published by Elsevier B.V.

1. Introduction

In the last 5 years, the introduction of cluster ion beams, particularly C_{60}^+, has put secondary ion mass spectrometry (SIMS) in the spotlight because of the increased sensitivity and reduced damage depth, which has opened up the possibility of three-dimensional imaging through the combination of lateral imaging with depth profiling [1–6]. Applications range from the analysis of multilayered inorganic materials [5] to the molecular depth profiling of sections of brain tissue [4]. However, the reactive nature of carbon atoms in the projectile may introduce unexpected processes that limit its usefulness. For example, depth profiling experiments of C_{60}^+ on silicon by Gillen et al. indicates unusual behavior that is unique to the pairing of the projectile and the target material [7]. At low incident kinetic energies, the sputtering yield is extinguished while, at higher incident kinetic energies, accumulation of material deposited on the surface results in the production of carbon deposits with unusual surface topography. Kozole and Winograd have also observed the formation of large C mound-like deposits in depth profiling experiments of Si with C_{60}^+ [8].

Previous molecular dynamics simulations (MD) of the bombardment of Si with normal incident keV C_{60} projectiles have explained the origin of the peculiar behavior observed in these experiments [9]. Strong covalent bonds are formed between C atoms from the projectile and Si atoms in the solid, which result in nearly all of the C atoms from the projectile being deposited into the target. The yield of sputtered Si atoms increases with incident kinetic energy until it exceeds the number of deposited C atoms. Consequently, the simulations reproduce the experimental observation of a transition from net deposition to net erosion of material. The transition occurs at ~12 keV in the simulations, which is comparable to the estimated value of ~14.5 keV in the depth profiling SIMS experiments [7], even though the simulations model a single impact event on the surface.

In previous work, simulations of C_{60} keV bombardment of different Si and C containing substrates were performed in order to see how the sputtered yield depends on the chemical composition and structure of the substrate [10,11]. The focus of this study is to understand how chemical bond formation between projectile atoms and target atoms alters the net sputtered yield of atoms in keV C_{60} bombardment of Si. Simulations of C_{60} keV bombardment of Si are modified by removing the chemistry and the results are compared with those from the C_{60} projectile containing the reactive C atoms. In order to mimic the MD simulations with C_{60} while

* Corresponding author. Tel.: +1 843 953 3378; fax: +1 843 953 1404.
E-mail address: krantzmank@cofc.edu (K.D. Krantzman).

0168-583X/$ - see front matter Published by Elsevier B.V.
doi:10.1016/j.nimb.2008.11.055

also removing the effects of bond formation, an artificial Ne_{60} cluster is used, which is composed of non-reactive Ne atoms that cannot form bonds with the atoms in the Si target. In order to separate the effect of the mass of the projectile atoms from the chemistry, simulations are also performed with $^{12}Ne_{60}$ clusters that are composed of Ne atoms with an artificial mass equal to that of C. The sputtered yield of Si atoms is greater with both the Ne_{60} and $^{12}Ne_{60}$ clusters than with C_{60}. We present a detailed mechanistic study to analyze why the sputtered yield is greater with the Ne_{60} and $^{12}Ne_{60}$ projectiles. The mesoscale energy deposition footprint (MEDF) model [12–14] is applied to understand how the sputtered yield depends on two characteristics of the projectile atoms, the chemical reactivity and the mass.

2. Description of the simulations

The classical method of MD is used to model the systems of interest, and the application of this method to keV bombardment of solids is explained comprehensively elsewhere [15,16]. Specifics of the application of the method to these particular simulations are reported elsewhere and include detailed descriptions of the microcrystallite used to model the Si target, the potentials used to describe the interactions between the atoms, and the heat bath used to minimize edge effects [11]. Four trajectories at impact points chosen from the center of the crystal were calculated for a time of 10 ps at each kinetic energy with each projectile. Only a few trajectories are needed in order to obtain a qualitative assessment of the trends in the sputtered yields.

An empirical many body potential developed by Tersoff [17] is used to model the Si–Si, C–C and Si–C interactions. The Ne–Ne interactions are described by a Lennard Jones 12-6 potential with $\varepsilon = 0.00405$ eV and and $\sigma = 2.7$ Å [18]. Purely repulsive Molière potentials are used to model the Ne–Si interactions. The same potentials are used to describe the interactions for the simulations with $^{12}Ne_{60}$, but the mass of carbon is used for the Ne atoms. Although the positions of the atoms in the Ne clusters are not equal to the equilibrium values, the projectile remains unaltered until it impacts the surface. The difference in the potential energy of the Ne atoms compared to the potential of energy of the C atoms in the projectile is negligible in comparison to the initial kinetic energy of bombardment.

3. Results and discussion

The beginning of the discussion focuses on how the number of sputtered Si atoms and number of deposited projectile atoms depends on both the projectile and the incident kinetic energy. The net sputtered yield is calculated as the difference between the number of sputtered Si atoms and the number of deposited projectile atoms and is plotted for all three projectiles as a function of incident kinetic energy. The MEDF model is used to examine the energy deposition footprints in the substrate that are produced by the impacts of the 20 keV C_{60}, Ne_{60} and $^{12}Ne_{60}$ projectiles. The footprints can be understood by comparison with snapshots of the initial pathway of the projectile atoms through the substrate during the first 200 fs of bombardment in the trajectory. Finally, the MEDF predicted yields for the one trajectory at 20 keV are calculated from the volume of the energy footprint and compared with the sputtered yields obtained from the complete trajectories.

3.1. Net sputtered yields

In Table 1, the number of sputtered Si atoms and deposited projectile atoms from the keV normal incident bombardment of Si is shown for all three projectiles at incident kinetic energies ranging from 5 to 20 keV. In general, the number of sputtered Si atoms increases with increasing incident kinetic energy with all three projectiles. When compared to the results with C_{60}, both the Ne_{60} and $^{12}Ne_{60}$ projectiles produce a large increase in the number of sputtered Si atoms at all incident kinetic energies. The sputtered yield with $^{12}Ne_{60}$ is greater than with the heavier Ne atoms in Ne_{60}. The relative increase in yield with both the Ne_{60} and $^{12}Ne_{60}$ projectiles decreases as the incident kinetic energy increases, ranging from a factor of 6 at 5 keV to a factor of only 1.5 at 20 keV. The results show that chemical bonding between the projectile atoms and the target atoms reduces the sputtered yield, and this factor becomes less important at higher incident kinetic energies.

Nearly all of the C atoms from the C_{60} projectile are deposited in the target at all incident kinetic energies, while only a third of the projectile atoms are left remaining in the solid with the Ne_{60} and $^{12}Ne_{60}$ clusters. An important difference, however, is that the implanted C atoms are chemically bonded to substrate atoms in the surface. Although ^{12}Ne and C have the same mass, 70% of the ^{12}Ne atoms are reflected back into the vacuum. Therefore, it is clear that the primary reason for the large deposition of C atoms into Si is due to the formation of strong covalent bonds. The number of projectile atoms backscattered into the vacuum is independent of the incident kinetic energy.

In Fig. 1, the net number of sputtered atoms is plotted for all three projectiles as a function of incident kinetic energy. The transition from net deposition to net erosion occurs when the net sputtered yield becomes greater than zero. Both Ne_{60} and $^{12}Ne_{60}$ have a greater sputtered yield of Si atoms than C_{60} and also have fewer atoms remaining in the substrate. Consequently, the differences in the net sputtered yield are more pronounced than the difference in the sputtered yields of Si atoms with the three projectiles. The average net sputtered yield with $^{12}Ne_{60}$ is greater than that with Ne_{60}, but the values are comparable within the standard deviations from the averages. Therefore, the effect of removing the chemistry is more important than the mass of the projectile atoms. The transition from net deposition to net erosion occurs at a lower value of incident kinetic energy, ~2 keV, with Ne_{60} and $^{12}Ne_{60}$ than the value of ~12 keV with C_{60}. The net sputtered yield is significantly greater with the Ne_{60} and $^{12}Ne_{60}$, and is a factor of two to three times greater at 15 and 20 keV.

Table 1
Average yield and standard deviation of sputtered and deposited atoms from C_{60}, Ne_{60} and $^{12}Ne_{60}$ bombardment of Si.

Incident kinetic energy (keV)	C_{60}		Ne_{60}		$^{12}Ne_{60}$	
	Sputtered atoms	Deposited atoms	Sputtered atoms	Deposited atoms	Sputtered atoms	Deposited atoms
5	8 ± 4	58 ± 2	47 ± 20	13 ± 4	44 ± 9	16 ± 1
8	25 ± 9	55 ± 2	61 ± 13	14 ± 2	97 ± 23	12 ± 2
10	44 ± 17	56 ± 0	86 ± 17	15 ± 2	114 ± 27	15 ± 2
12	62 ± 17	55 ± 1	113 ± 35	18 ± 1	171 ± 23	16 ± 4
15	97 ± 28	55 ± 1	135 ± 18	13 ± 2	158 ± 36	19 ± 4
20	146 ± 33	55 ± 2	212 ± 36	18 ± 2	237 ± 30	23 ± 2

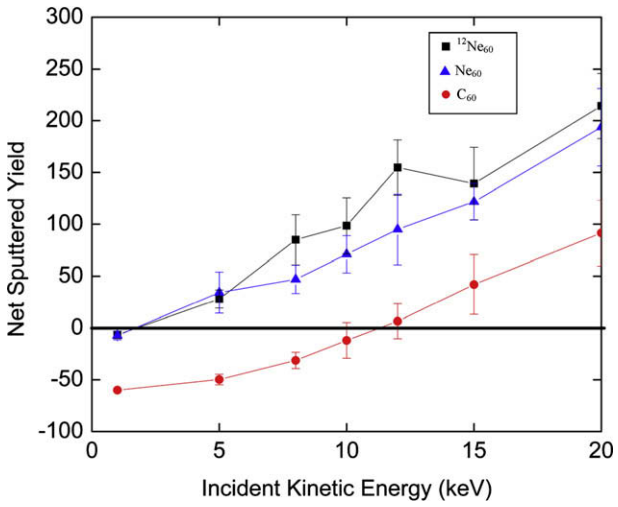

Fig. 1. Average net sputtered yields from the simulations are plotted as a function of incident kinetic energy for the three projectiles, $^{12}Ne_{60}$ (squares), Ne_{60} (triangles) and C_{60} (circles). The error bars shown for each number are the standard deviation from the average over a set of four trajectories.

3.2. Application of the MEDF model

An analysis of the simulations by the MEDF model gives physical insight into the reasons for the higher net sputtered yields with Ne_{60} and $^{12}Ne_{60}$. The basic ideas and application of the model to simulations of keV bombardment are described in detailed elsewhere [12–14]. The model is based on the work of Jakas et al. [19], and treats the bombardment induced particle ejection by two-dimensional fluid-dynamics. Briefly, the model assumes that the distribution of energy deposited by the projectile very early on in the bombardment process can be used to determine the sputtered yield at much later times. Initially, an energized cylindrical track with a characteristic radius, R_{cyl}, is created. Only particles near the surface at a depth of R_{cyl} or less will be ejected. As atoms are ejected into the vacuum, a wider surface area is exposed, and further ejection occurs from a surface area with radius $R_s = (\widetilde{E})^{1/2}R_{cyl}$, where $\widetilde{E}$ is the average excitation energy of the substrate atoms relative to the cohesive energy, U_0. The footprint from the projectile is equal to the volume of a cone with radius R_s and depth R_{cyl}. The volume of the footprint, along with the number density of the substrate, n_0, can be used to estimate the sputtering yield, $Y = n_0(\pi/3)R_s^2R_{cyl}$, which simplifies to $Y = n_0(\pi/3)R_{cyl}^3\widetilde{E}$.

The distribution of energy deposition in the substrate is analyzed for all three projectiles at an incident kinetic energy of 20 keV. In Fig. 2, contour plots of the excitation energy relative to the cohesive energy, $\widetilde{E}/U_0$, are plotted for each projectile. Each contour plot is centered in a 20-Å slice around the impact area and is drawn at the time when the projectile has lost 90% of its initial energy, which occurs at 90 fs for C_{60} and 110 fs for Ne_{60} and $^{12}Ne_{60}$. The value of R_{cyl} is estimated from the boundary around the region where atoms have enough energy to overcome the cohesive energy and is estimated to be 16 Å for each projectile. The average excitation energy per atom, $\widetilde{E}$, of the substrate atoms within a cylinder of radius and depth equal to R_{cyl} is calculated to be 1.3. The basis radius R_s, of the final ejection cone is calculated from the values of R_{cyl} and $\widetilde{E}$, and is estimated to be 18 Å with all three projectiles.

The similarity in the energy distribution between the three projectiles can be understood by an analysis of the motion of the projectile as it impacts the surface. In Fig. 3, the motion of the projectile atoms from 0 to 200 fs at 10 fs intervals are overlaid on a single time snapshot of the position of the substrate atoms at 200 fs. A comparison of snapshots of the initial pathway of the projectile atoms through the substrate show that all three projectiles have a similar lateral and vertical distribution that is centered in the region of the energy footprint. The majority of particles travel through this lateral region and some particles move deeper into the crystal below a depth of R_{cyl}. The only notable difference between the snapshots is the number of backscattered atoms. $^{12}Ne_{60}$ has the greatest number of backscattered projectile atoms, while C_{60} has the smallest number. It is not surprising that the energy distribution is similar for all three projectiles, because the pathways of the projectile atoms through the substrate are similar.

The formula derived from the MEDF model is used to calculate the predicted yield for the same trajectory for each projectile that is analyzed in Figs. 2 and 3. As shown in Fig. 2, the volume of the ejection cone with each projectile is the same, and has a value of 5×10^3 Å^3. When multiplied by the number density of Si, 0.050 atoms/Å^3, the MEDF predicted yield is 2.7×10^3. The MEDF model predicts the same yield for all three projectiles, because the initial energy distributions are similar. This agreement in

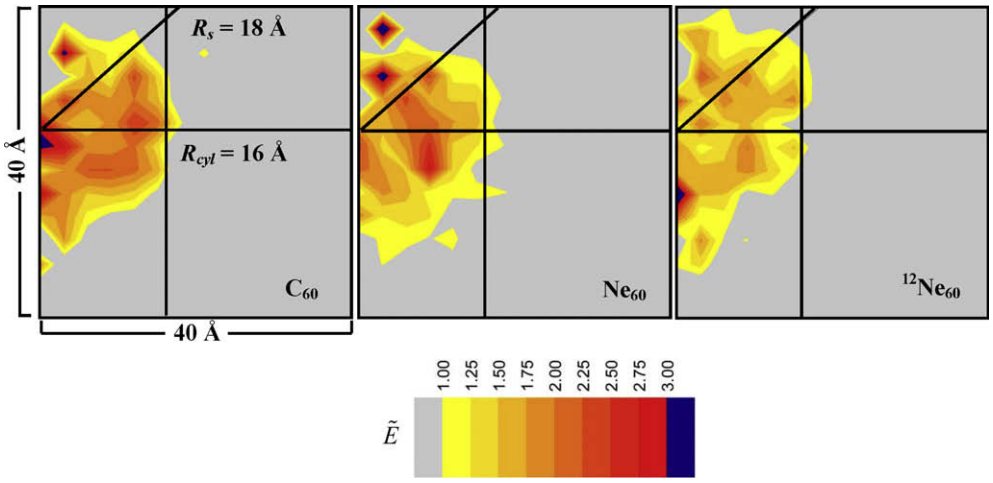

Fig. 2. Contour plots of the excitation energy for the 20 keV bombardment of Si with the C_{60}, Ne_{60} and $^{12}Ne_{60}$ projectiles. Each contour plot corresponds to a single trajectory and has the same dimensions, a radial distance of 40 Å from the impact point and a depth of 40 Å from the top of the substrate. The boundary between the white and shaded regions outlines the region in which there is sufficient energy to overcome the cohesive energy. Values of the radius of the energized cylindrical track, R_{cyl}, are estimated from the position of this boundary. The value of R_{cyl} is estimated to be 16 Å for each projectile. The vertical and horizontal lines are drawn at the estimated value of R_{cyl}, 16 Å. The diagonal lines outline the ejection cones with an estimated radius of R_s of 18 Å and depth equal to R_{cyl}.

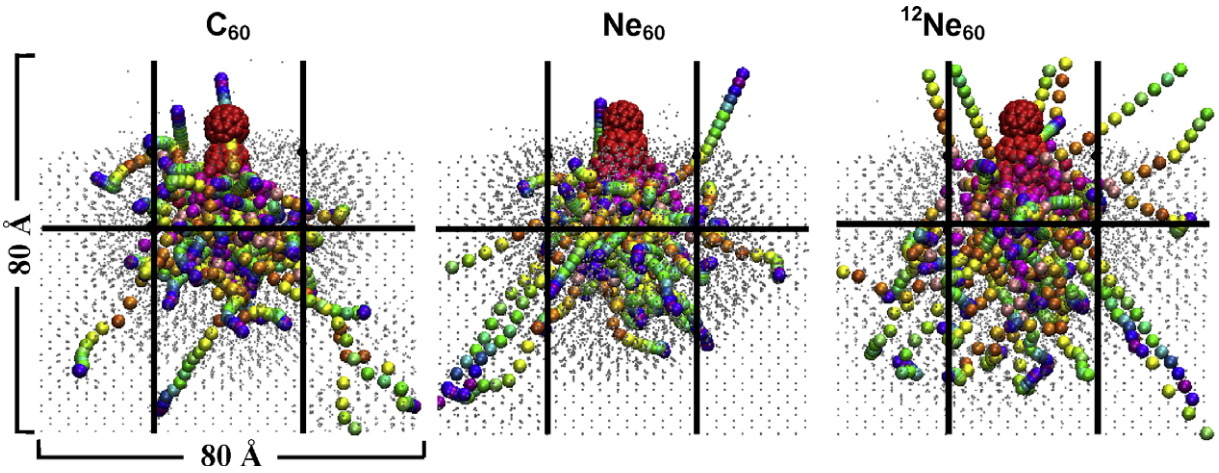

Fig. 3. Time snapshots of the projectile collision events at 200 fs for 20 keV bombardment of Si with the C_{60}, Ne_{60} and $^{12}Ne_{60}$ projectiles. The projectile atoms are shown as solid spheres, and the positions of the atoms are plotted at 10 fs intervals from 0 to 200 fs. The atoms are shaded in gray tones to differentiate the positions of atoms at each time. The horizontal lines outline the lateral region centered 16 Å from the impact point and the vertical line is drawn at a depth equal to 16 Å from the top of the substrate.

predicted yields reflects the basic assumptions of the MEDF model that the source of the initial energy does not participate in the subsequent fluid flow dynamics. Although the MEDF model overestimates the yield of sputtered Si atoms for all three projectiles, the greatest discrepancy is for the C_{60} projectile. In this case, the MEDF model overestimates the number of sputtered Si atoms by a factor of 2. The reason for the poor agreement with C_{60} is that the incident particles attach themselves chemically to the substrate atoms and inhibit ejection more than the inert Ne projectiles.

4. Conclusions

Simulations of C_{60} bombardment of Si and C containing substrates show that strong covalent bonds can form between the projectile atoms and atoms in the target material, which results in the majority of C atoms being incorporated into the substrate lattice. When the effect of chemistry is removed by using Ne_{60} and $^{12}Ne_{60}$ clusters, the sputtered yield is significantly greater. The net sputtered yield with both the Ne_{60} and $^{12}Ne_{60}$ clusters is similar, and therefore, the mass of the projectile atoms is not as important as the chemistry between the projectile and target atoms. When reactive C atoms are in the bombarding projectile, the C atoms bond to Si atoms, which keeps them in the substrate rather than eject them. Therefore, chemical bonding reduces the yield of sputtered Si atoms.

Acknowledgements

B.J.G. acknowledges financial support for this research through the Chemistry Division of the National Science Foundation under Grant CHE-0456514. K.D.K. acknowledges financial support from a Research and Development Grant from the College of Charleston as well as financial support from the Department of Chemistry and Biochemistry at the College of Charleston.

References

[1] N. Winograd, Anal. Chem. 77 (2005) 142A.
[2] A. Wucher, J. Cheng, N. Winograd, Anal. Chem. 79 (2007) 5529.
[3] J. Cheng, A. Wucher, N. Winograd, J. Phys. Chem. B 110 (2006) 8329.
[4] E.A. Jones, N.P. Lockyer, J.C. Vickerman, Anal. Chem. 80 (2008) 2125.
[5] S. Sun, A. Wucher, C. Szakal, N. Winograd, Appl. Phys. Lett. 84 (2004) 5177.
[6] G. Gillen, A. Fahey, M. Wagner, C. Mahoney, Appl. Surf. Sci. 252 (2006) 6537.
[7] G. Gillen, J. Batteas, C.A. Michaels, P. Chi, J. Small, E. Windsor, A. Fahey, J. Verkouteren, K.J. Kim, Appl. Surf. Sci. 252 (2006) 6521.
[8] J. Kozole, D. Willingham, N. Winograd, The effect of incident angle on the C_{60}^{+} bombardment of molecular solids, Appl. Surf. Sci. (2007), doi:10.1016/j.apsusc.2008.05.254.
[9] K.D. Krantzman, D.B. Kingsbury, B.J. Garrison, Appl. Surf. Sci. 252 (2006) 6463.
[10] K.D. Krantzman, R.P. Webb, B.J. Garrison, Simulations of C_{60} bombardment of Si, SiC, diamond and graphite, Appl. Surf. Sci. (2008), doi:10.1016/j.apsusc.2008.05.236.
[11] K.D. Krantzman, B.J. Garrison, J. Phys. Chem., accepted for publication.
[12] M.F. Russo Jr., B.J. Garrison, Anal. Chem. 78 (2006) 7206.
[13] M.F. Russo Jr., C. Szakal, J. Kozole, N. Winograd, B.J. Garrison, Anal. Chem. 79 (2007) 4493.
[14] K.E. Ryan, M.F. Russo Jr., E.J. Smiley, Z. Postawa, B.J. Garrison, Combined simulations and analytical model for predicting trends in cluster bombardment, Appl. Surf. Sci. (2008), doi:10.1016/j.apsusc.2008.05.084.
[15] B.J. Garrison, in: J.C. Vickerman, D. Briggs (Eds.), ToF-SIMS: Surface Analysis by Mass Spectrometry, Surface Spectra, Manchester, 2001, p. 123.
[16] B.J. Garrison, Z. Postawa, Mass. Spectrom. Rev. 27 (2008) 289.
[17] J. Tersoff, Phys. Rev. B 39 (1989) 5566.
[18] M.P. Allen, D.J. Tildesley, Computer Simulations in Liquids, Oxford University Press, Oxford, 1987.
[19] M.M. Jakas, E.M. Bringa, R.E. Johnson, Phys. Rev. B 65 (2002) 165425.